Electronic Supplementary Material (ESI) for Dalton Transactions.

Mechanochemical Routes for the Synthesis of acetyl- and bis-(imino)pyridine Ligands and Organometallics

Thomas E. Shaw, Lorianne R. Shultz, Louiza R. Garayeva, Richard G. Blair, Bruce C. Noll, Titel Jurca*

SUPPORTING INFORMATION

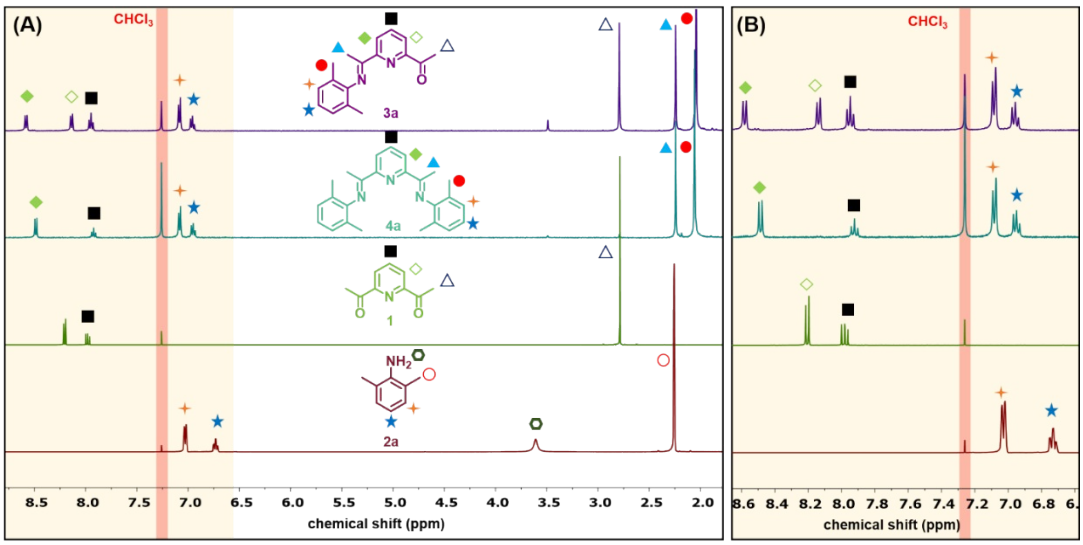

Figure S1: ^{1}H NMR spectra in $CDCl_3$ of starting reagents **1** and **2a**, and isolated products **3a** and **4a**; (*right*) highlighted downfield aromatic region used for product distribution determination via the integration of pyridine *meta*-CH peaks.

Optimization experiments:

Entry	Time (h)	Ball (SS)	$MgSO_4$ (mg)	TsOH (mg)	MeOH (mL)	Yield (^{1}H NMR) 3a	4a
1	1	1 x 1/8in	-	-	-	0%	0%
2	1	1 x 1/8in	-	10	-	45%	8%
3	1	1 x 1/4in	-	10	-	43%	7%
4	1	4 x 1/8in	-	10	-	46%	10%
5	1	1 x 1/8in	-	-	0.1	0%	0%
6	1	1 x 1/8in	100	10	-	50%	16%
7	1	1 x 1/8in	-	25	-	42%	6%
8	1	1 x 1/8in	-	5	-	39%	5%
9	1	1 x 1/8in	250	10	-	48%	14%
10	1	1 x 1/8in	-	10	0.1	44%	9%
11	1	1 x 1/8in	100	-	-	0%	0%
12	1	1 x 1/8in	100	10	0.1	48%	16%
13	1	1 x 1/8in	*100	10	-	41%	8%
14	3	4 x 1/8in	100	10	-	25%	67%
@15	4	4 x 1/8in	200	10	-	17%	80%

* = Celite® 545

@ = 1 = 200 mg vs 300 mg for entries 1-14

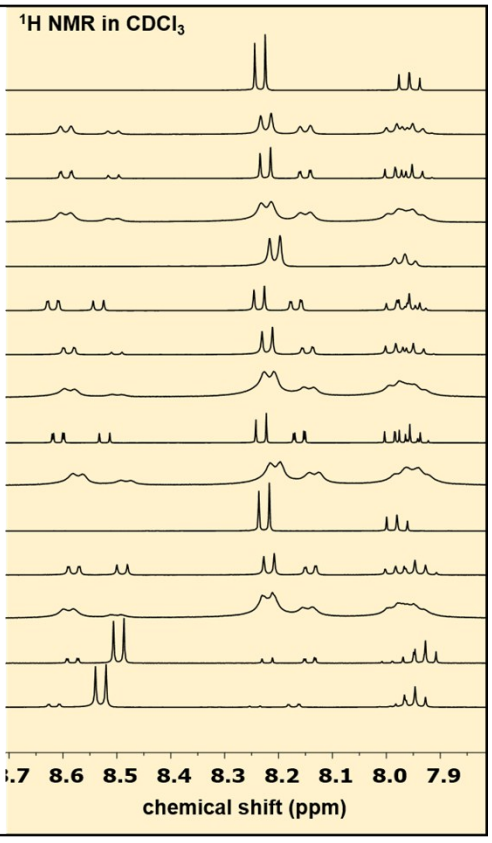

Figure S2: (*left*) optimization table for the reaction of **1** and **2a** with various additives: TsOH = *p*-toluenesulfonic acid monohydrate; (*right*) corresponding downfield aromatic region from the ^{1}H NMR spectra in $CDCl_3$ used for product distribution determination via the integration of pyridine *meta*-CH peaks.

Timed reactions:

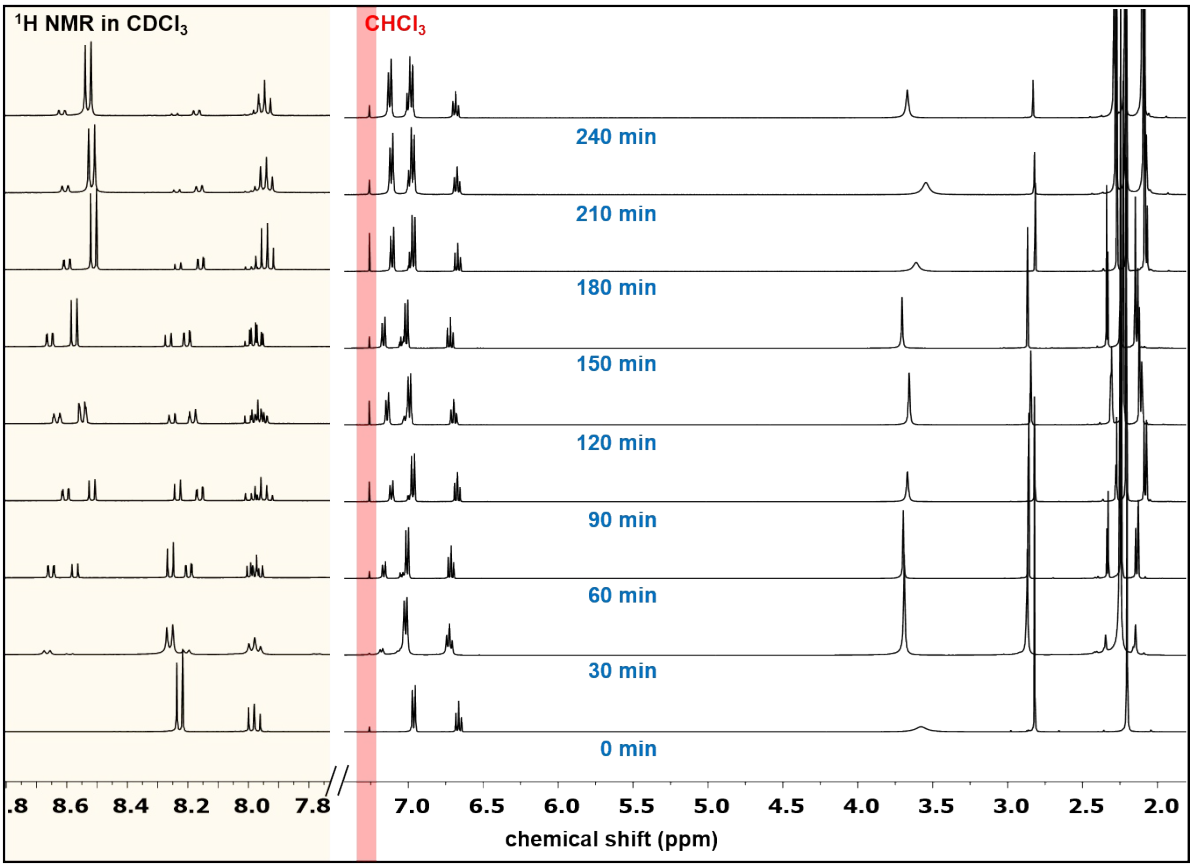

Figure S3: ^{1}H NMR spectra in $CDCl_3$ for the optimized mechanochemical reaction of **1** and **2a** as a function of time. *Each measurement represents a discreet sample terminated at the note 30 minute intervals.*

Time (min)	*% 1*	*% 3a*	*% 4a*	*Temperature °C*
0	*100*	*0*	*0*	*21.7*
30	*70*	*27*	*3*	*35.3*
60	*35*	*49*	*16*	*38.9*
90	*23*	*51*	*26*	*43.7*
120	*14*	*46*	*40*	*41.6*
150	*13*	*44*	*43*	*40.2*
180	*11*	*43*	*46*	*37.2*
210	*4*	*26*	*70*	*38.1*

Table S1: % composition of reactions depicted in Figure S3 and additional corresponding temperature depicted in Figure 1 (manuscript).

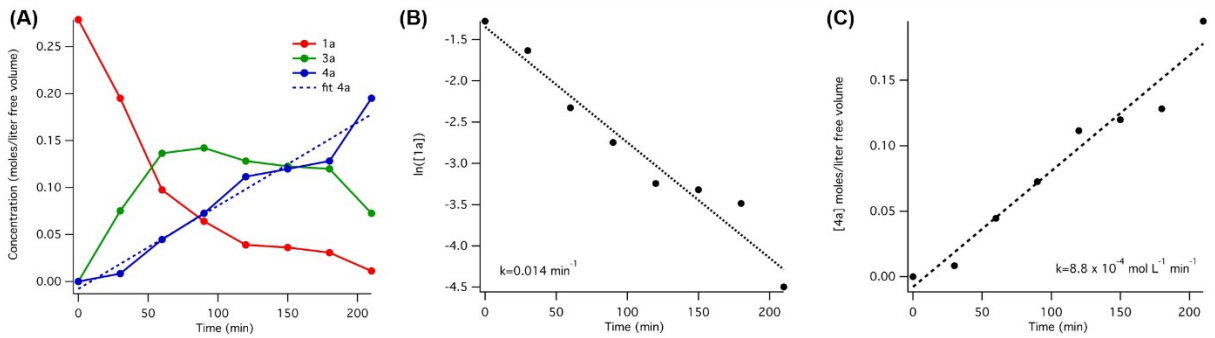

Figure S4: (A) Concentration vs free volume as a function of time for **1**, **3a**, and **4a**. (B) ln[**1a**] as a function of time reveals first order for **1a**. (C) Concentration of 4a as a function of time reveals a pseudo-zeroth order for **4a**.

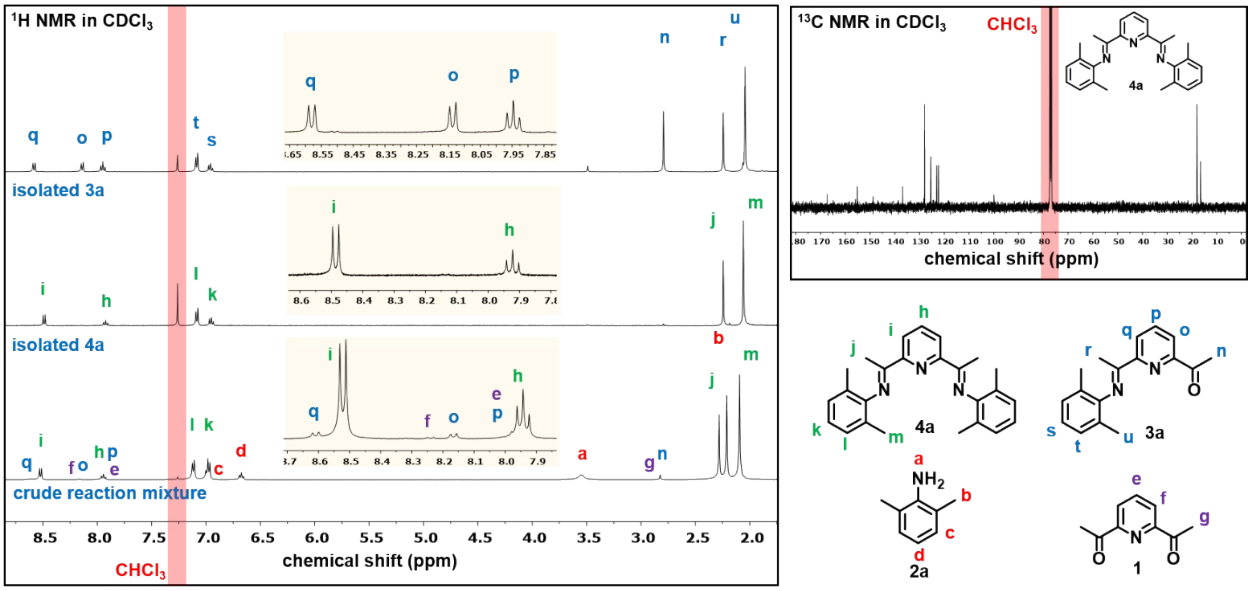

Figure S5: (*left*) ^{1}H NMR spectra in $CDCl_3$ for the crude reaction mixture from the mechanochemical reaction of **1** and **2a** with $MgSO_4$ and TsOH, and isolated products **3a** and **4a** after workup. (*right*) ^{13}C NMR in $CDCl_3$ of **4a**.

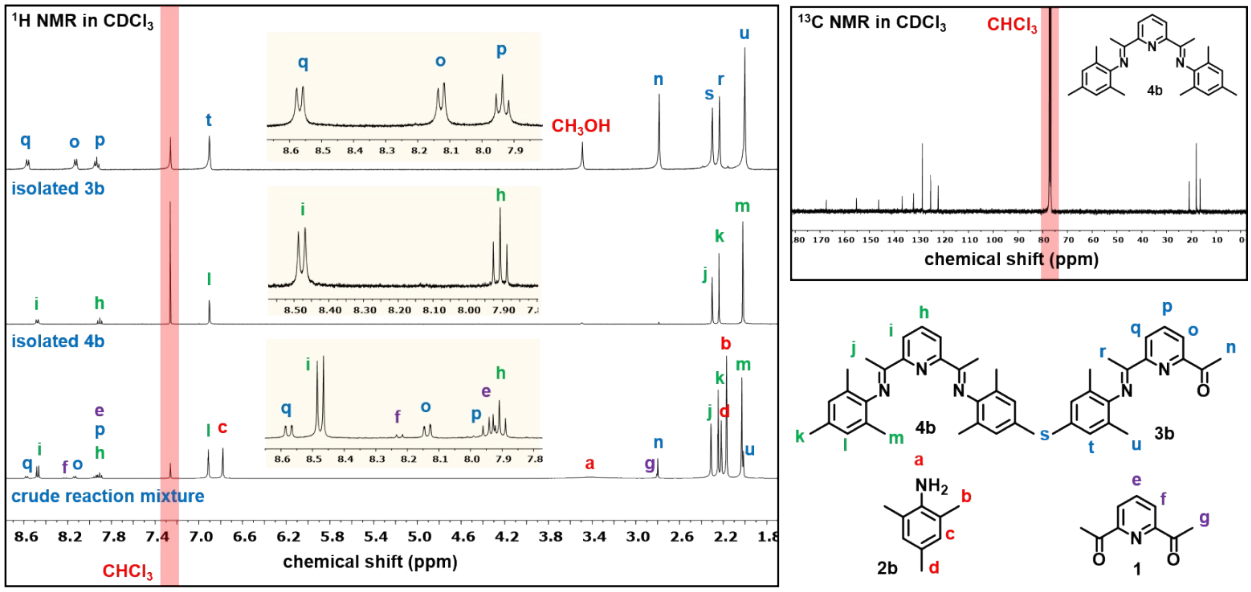

Figure S6: (*left*) ^{1}H NMR spectra in $CDCl_3$ for the crude reaction mixture from the mechanochemical reaction of **1** and **2b** with $MgSO_4$ and TsOH, and isolated products **3b** and **4b** after workup. *MeOH in the spectrum for **3b** is due to trace solvent of crystallization* (*right*) ^{13}C NMR in $CDCl_3$ of **4b**.

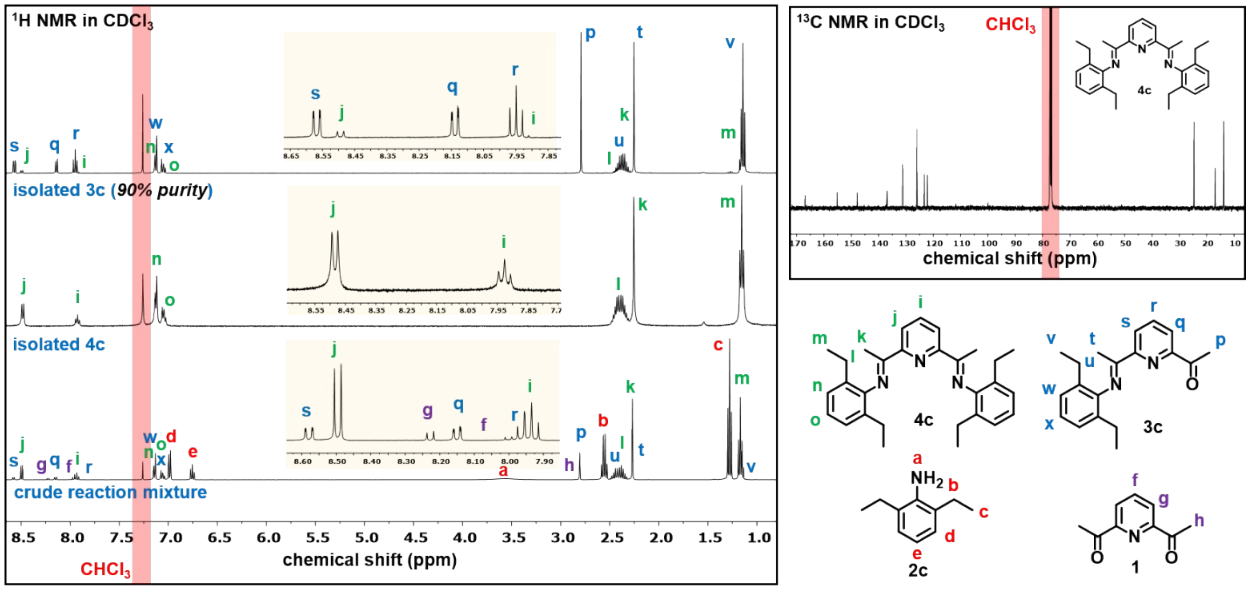

Figure S7: (*left*) ^{1}H NMR spectra in $CDCl_3$ for the crude reaction mixture from the mechanochemical reaction of **1** and **2c** with $MgSO_4$ and TsOH, and isolated products **3c** (*90% purity with 10% trace **4c***) and **4c** after workup. (*right*) ^{13}C NMR in $CDCl_3$ of **4c**.

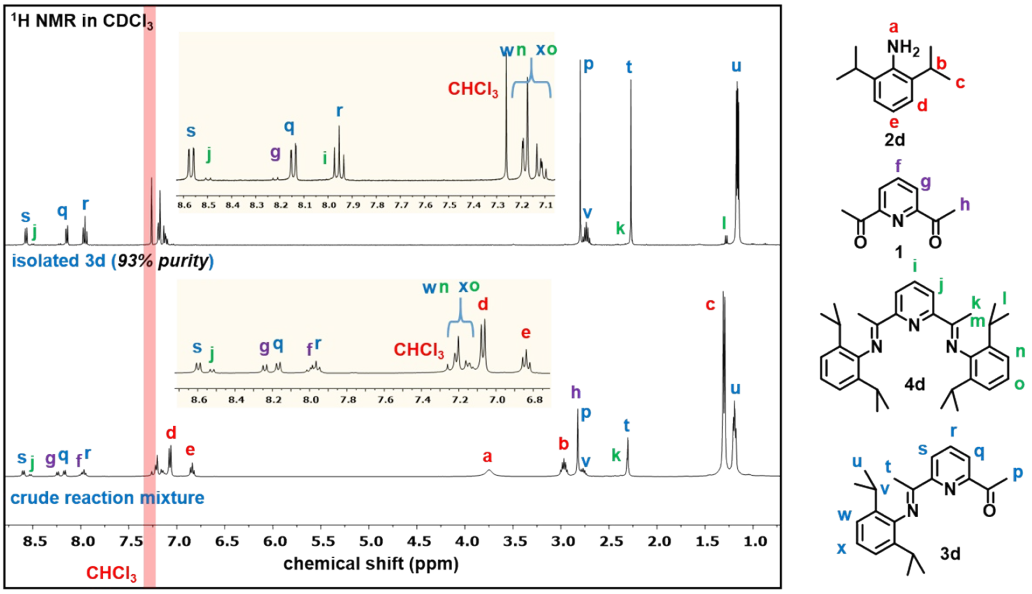

Figure S8: ^{1}H NMR spectra in $CDCl_3$ for the crude reaction mixture from the mechanochemical reaction of **1** and **2d** with $MgSO_4$ and TsOH, and isolated product **3d** (*93% purity*) with trace **4d** after workup.

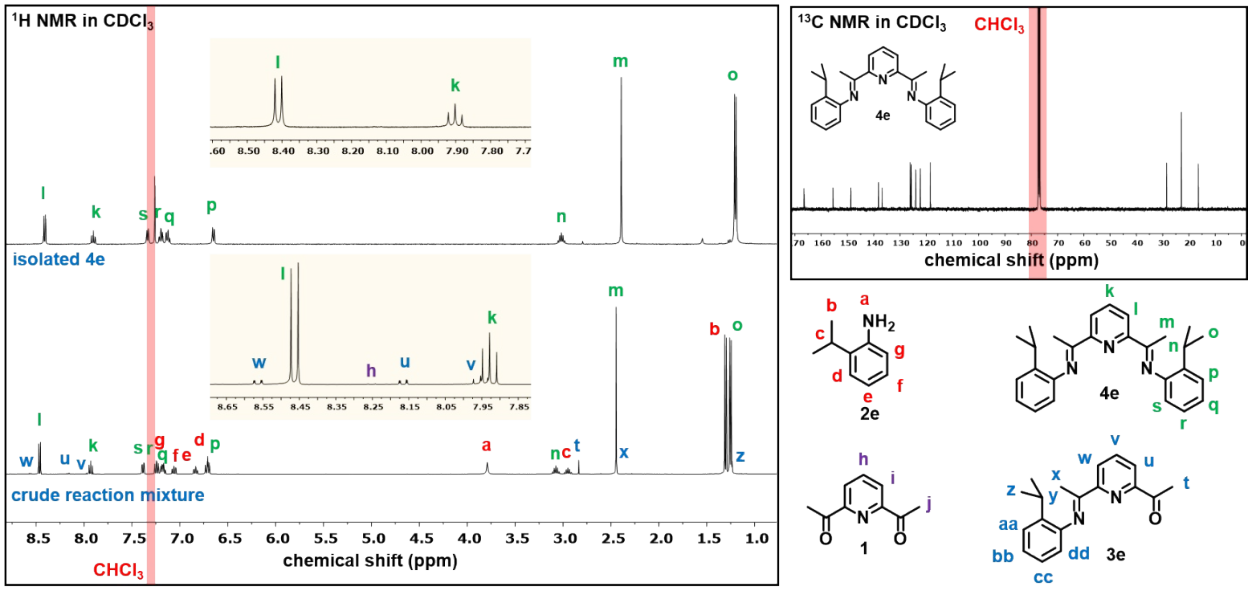

Figure S9: (*left*) ^{1}H NMR spectra in $CDCl_3$ for the crude reaction mixture from the mechanochemical reaction of **1** and **2e** with $MgSO_4$ and TsOH, and isolated product **4e** after workup. (*right*) ^{13}C NMR in $CDCl_3$ of **4e**.

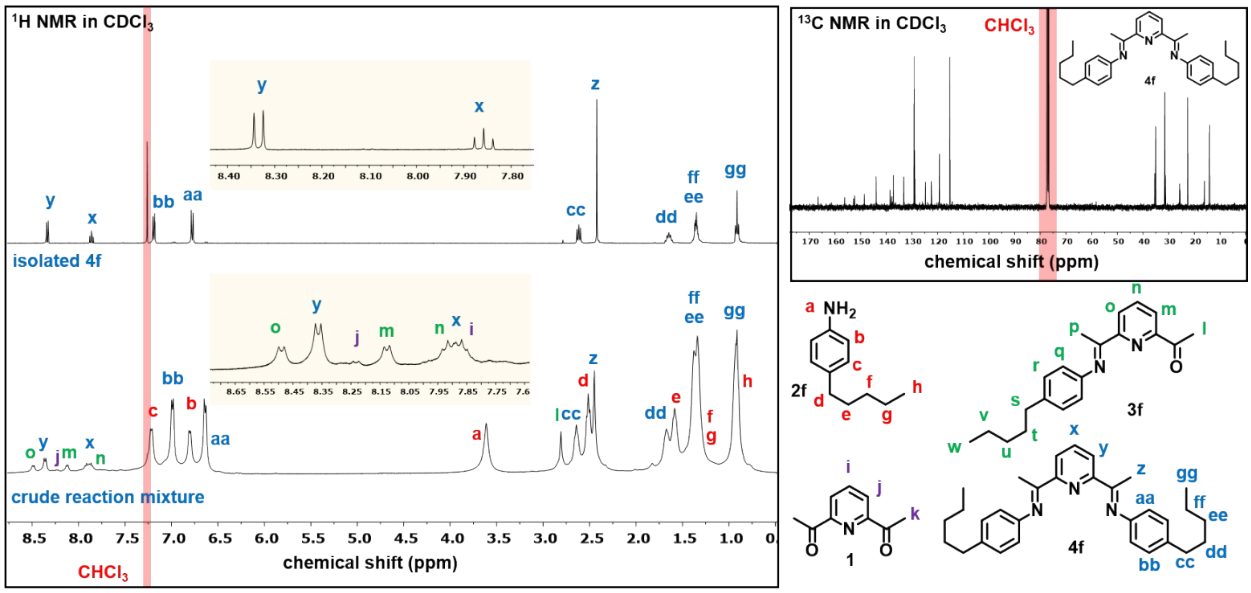

Figure S10: (*left*) ^{1}H NMR spectra in $CDCl_3$ for the crude reaction mixture from the mechanochemical reaction of **1** and **2f** with $MgSO_4$ and TsOH, and isolated product **4f** after workup. (*right*) ^{13}C NMR in $CDCl_3$ of **4f**.

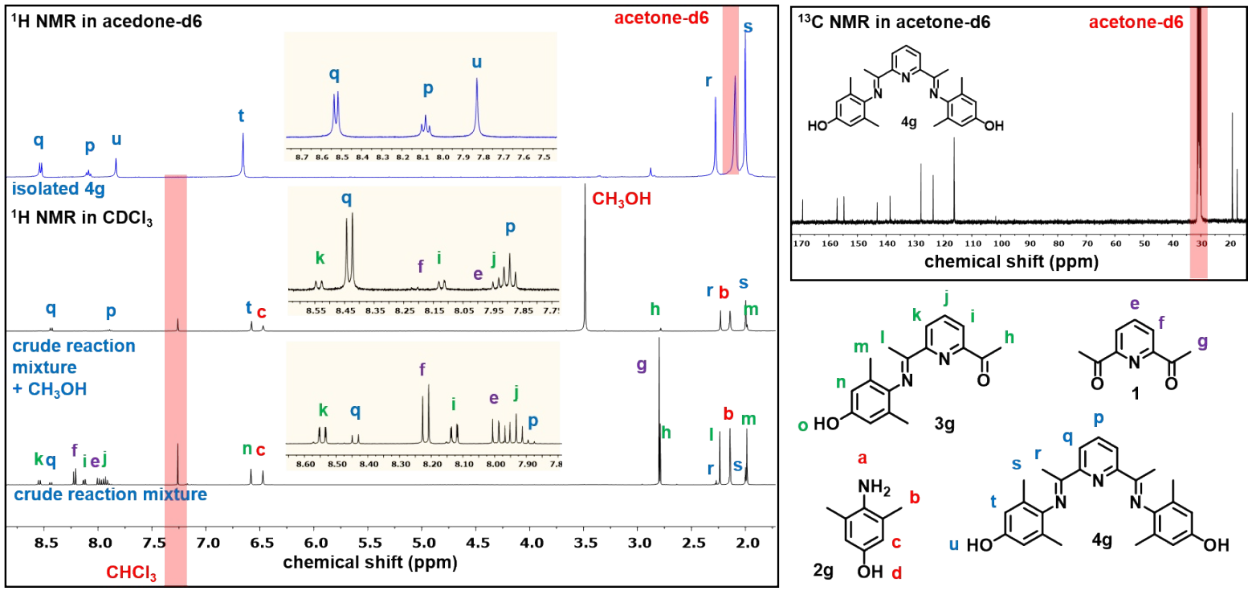

Figure S11: (*left*) ^{1}H NMR spectra in $CDCl_3$ for the crude reaction mixture from the mechanochemical reaction of **1** and **2g** with $MgSO_4$ and TsOH, and from the repeated reaction with methanol as additive, and isolated product **4g** after workup (*NMR in acetone-d6 for improved solubility*). (*right*) ^{13}C NMR in acetone-d6 of **4g**.

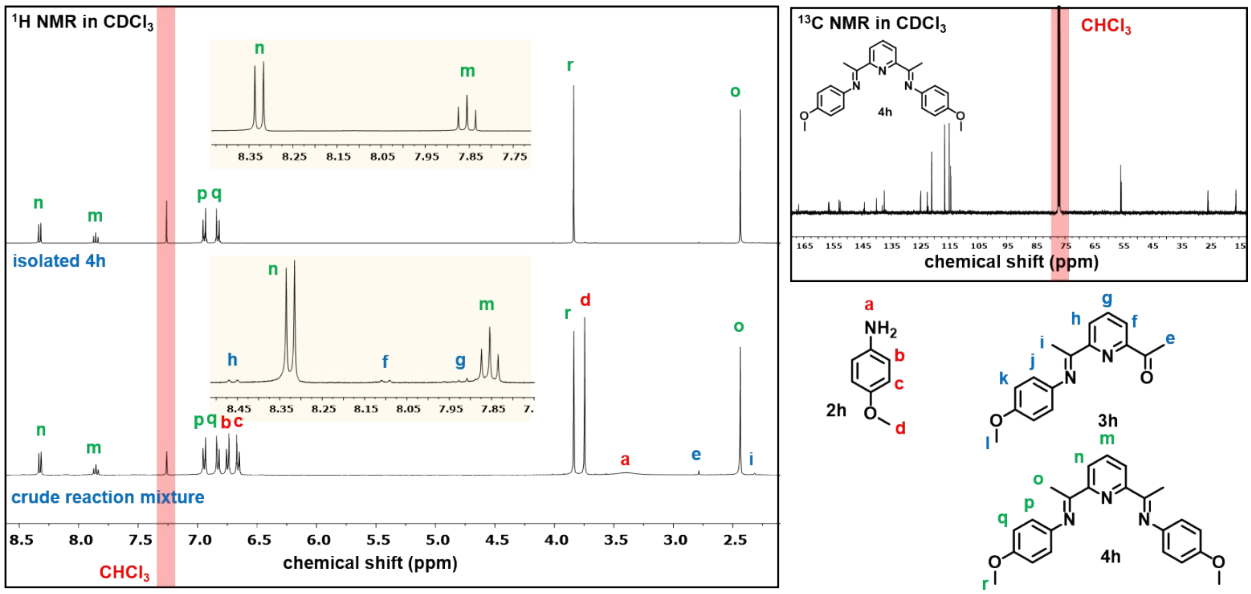

Figure S12: (*left*) ^{1}H NMR spectra in $CDCl_3$ for the crude reaction mixture from the mechanochemical reaction of **1** and **2h** with $MgSO_4$ and TsOH, and isolated product **4h** after workup. (*right*) ^{13}C NMR in $CDCl_3$ of **4h**.

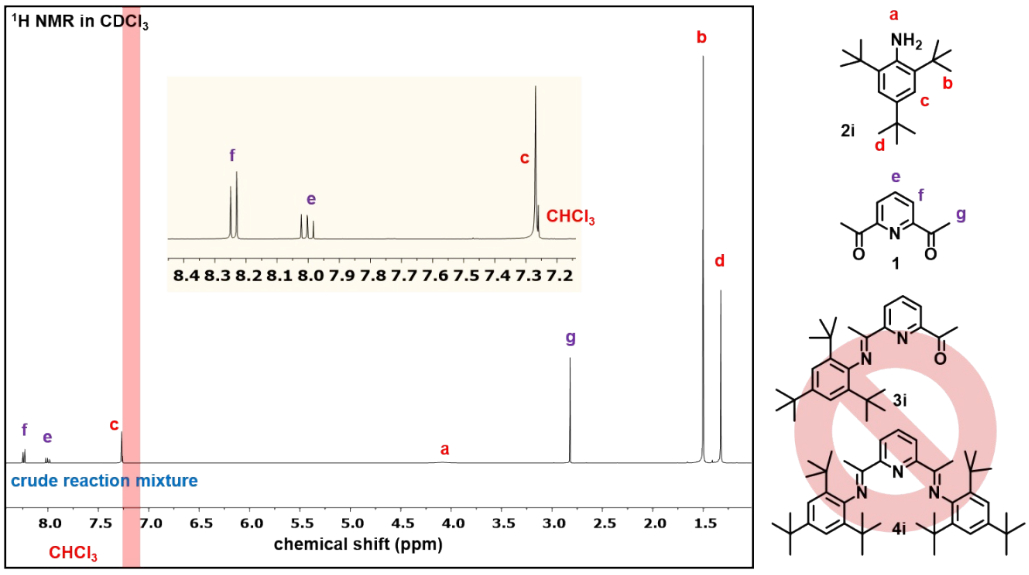

Figure S13: ^{1}H NMR spectrum in $CDCl_3$ for the crude reaction mixture from the *attempted* mechanochemical reaction of **1** and **2i** with $MgSO_4$ and TsOH.

General procedure for the scaled-up mechanochemical reaction of 1 with 2a or 2h:

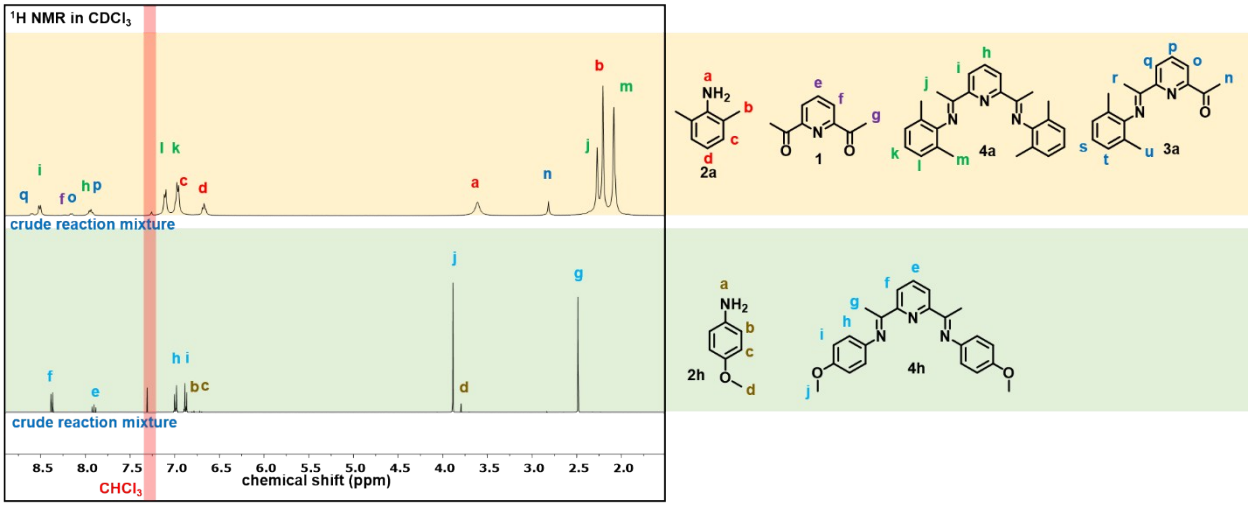

Figure S14: (*top*) ^{1}H NMR spectrum in $CDCl_3$ for the crude reaction mixture from the scaled-up mechanochemical reaction of **1** and **2a** with $MgSO_4$ and TsOH. (*bottom*) ^{1}H NMR spectrum in $CDCl_3$ for the crude reaction mixture from the scaled-up mechanochemical reaction of **1** and **2h** with $MgSO_4$ and TsOH.

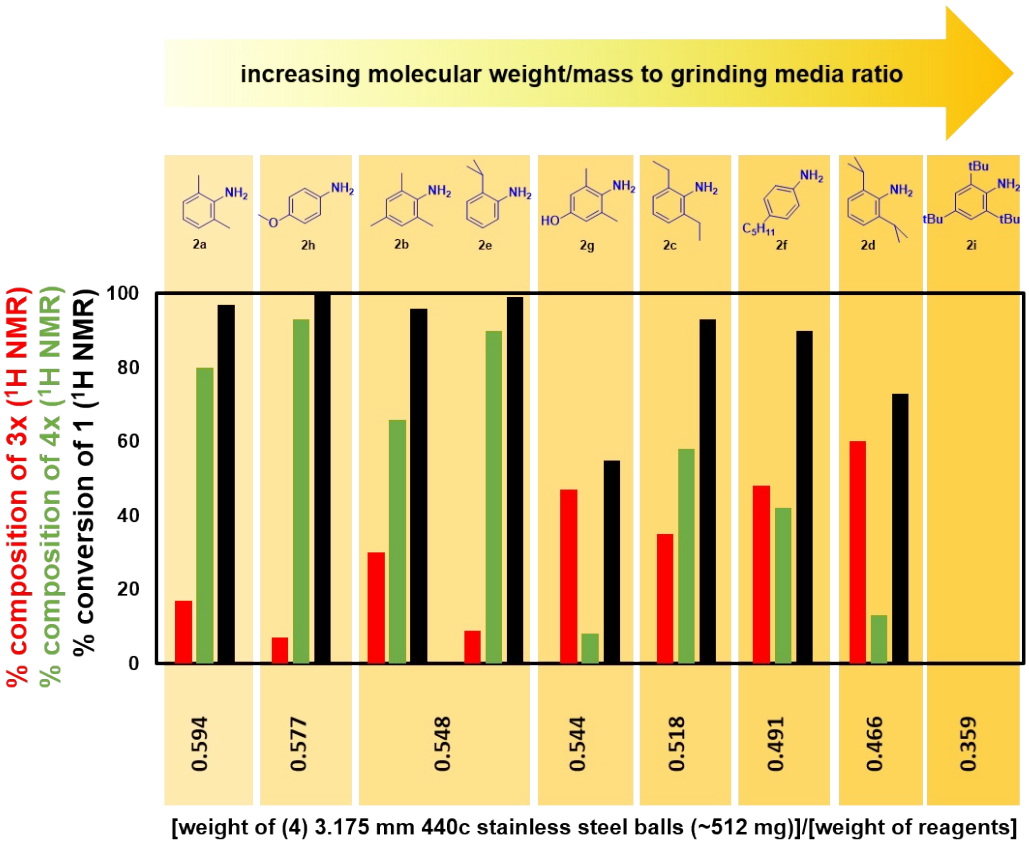

Figure S15: ball to reagent ratios in descending order (*left to right*) over the scope of anilines tested.

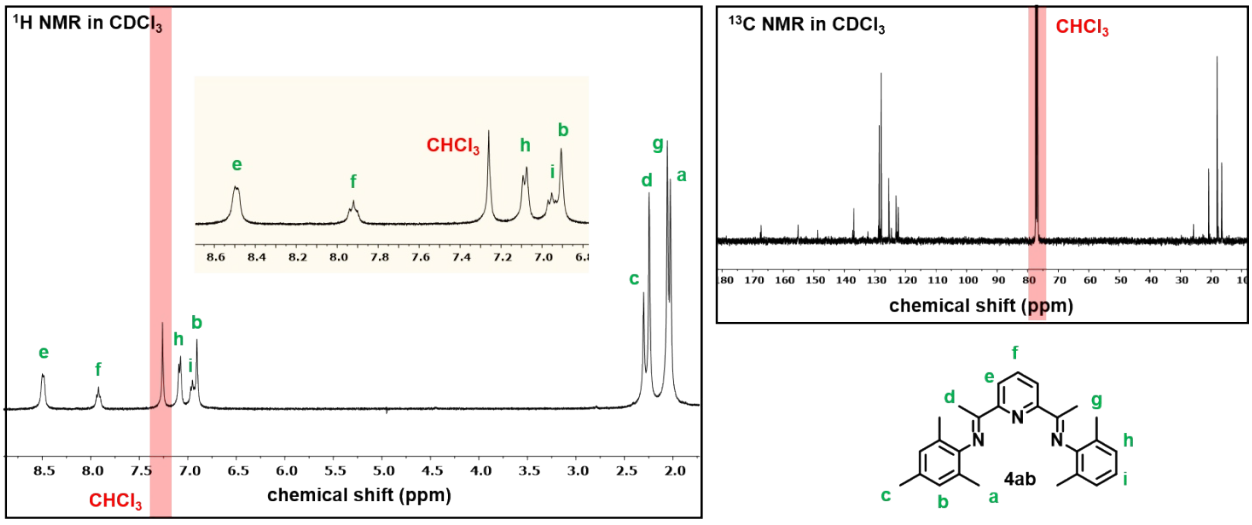

Figure S16: (*left*) ^{1}H NMR spectrum in $CDCl_3$ for the isolated products **4ab**. (*right*) ^{13}C NMR in $CDCl_3$ of **4ab**.

source	ligand	(i)	(ii)	(iii)	(iv)
This work	4a	0	19.6	4	69
Ref. 26a	4a	9.4	undisclosed	overnight (12+)	78
Ref. 14a	4a	22.4	undisclosed	Overnight (12+)	60
This work	4b	0	32.9	4	51
Ref. 26a	4b	11.4	undisclosed	overnight (12+)	60
Ref. 26b	4b	16.2	32.4	72	76

Table S2: Comparison of experimental protocols for the synthesis of **4a** and **4b**. (i) = reaction solvent (mL/g); (ii) workup solvent (mL/g); (iii) reaction time (h); (iv) % isolated yield.

Organometallic reactions

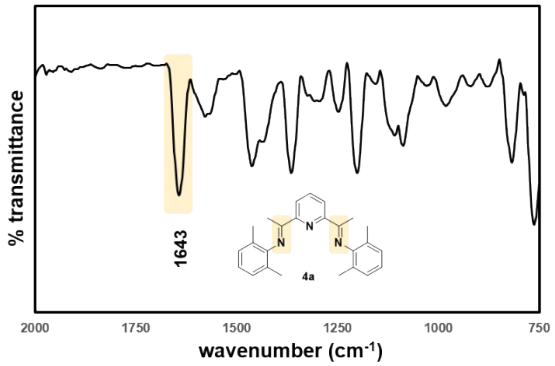

Figure S17: FTIR spectrum of **4a**.

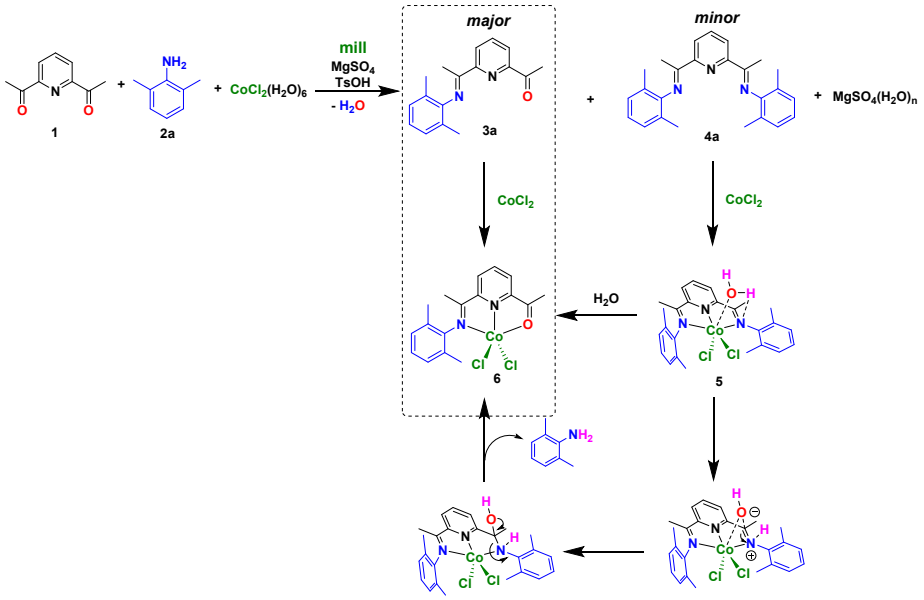

Scheme S1: proposed reaction sequence for **5** with H_2O to yield **6**.

Crystal structure report for 4ab:

A translucent pale gold plate-like specimen of $C_{26}H_{29}N_3$, approximate dimensions 0.046 mm x 0.126 mm x 0.148 mm was used for the X-ray crystallographic analysis. The X-ray intensity data were measured on a Bruker D8 VENTURE K-geometry diffractometer system equipped with a lncoatec lμS 3.0 microfocus sealed tube {Cu Ka, "A = 1.54178 A) and a multilayer mirror monochromator.

A total of 3853 frames were collected. The total exposure time was 17.00 hours. The frames were integrated with the Bruker SAINT software package using a narrow-frame algorithm. The integration of the data using a monoclinic unit cell yielded a total of 31948 reflections to a maximum 9 angle of 75.03° (0.80 A resolution), of which 4697 were independent (average redundancy 6.802, completeness = 99.1%, R_{int} = 5.96%, R_{sig} = 3.54%) and 4224 (89.93%) were greater than 2cr(F^2). The final cell constants of a = 8.0169(6) A, b = 12.0185(9) A, c = 23.9871(17) A, β = 90.409(3)°, volume = 2311.1(3) A^3, are based upon the refinement of the XYZ-centroids of 9891 reflections above 20 cr(I) with 7.355° < 29 < 149.2°. Data were corrected for absorption effects using the Multi-Scan method (SADABS). The ratio of minimum to maximum apparent transmission was 0.877. The calculated minimum and maximum transmission coefficients (based on crystal size) are 0.6608 and 0.7538.

The structure was solved and refined using the Bruker SHELXTL Software Package, using the space group P 1 21/c 1, with Z = 4 for the formula unit, $C_{26}H_{29}N_3$. The final anisotropic full-matrix least-squares refinement on F^2 with 280 variables converged at R1 = 5.98%, for the observed data and wR2 = 15.24% for all data. The goodness-of-fit was 1.080. The largest peak in the final difference electron density synthesis was 0.236 e^-/A^3 and the largest hole was -0.213 e^-/A^3 with an RMS deviation of 0.041 e^-/A^3. On the basis of the final model, the calculated density was 1.102 g/cm^3 and F(000), 824 e^-.

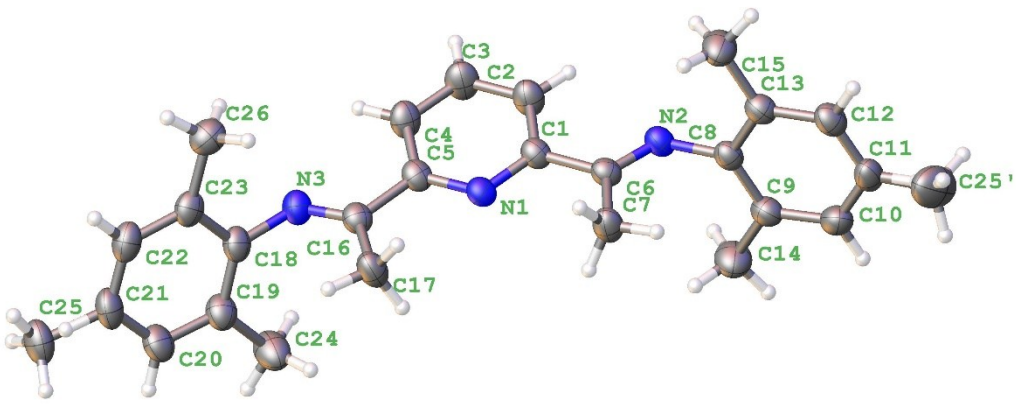

Figure S18: single crystal X-ray structure of **4a** with thermal ellipsoids drawn at the 50% probability level.

Table S3: Crystal data and structure refinement for 4ab

Empirical formula	$C_{26}H_{29}N_3$

Formula weight	383.52
Temperature/K	100.(2)
Crystal system	monoclinic
Space group	$P2_1/c$
a/Å	8.0169(6)
b/Å	12.0185(9)
c/Å	23.9871(17)
α/°	90
β/°	90.409(3)
γ/°	90
Volume/Å^3	2311.1(3)
Z	4
ρ_{calc}g/cm^3	1.102
μ/mm^{-1}	0.498
F(000)	824.0
Crystal size/mm^3	0.148 × 0.126 × 0.046
Radiation	Cu Kα (λ = 1.54178)
2Θ range for data collection/°	7.38 to 150.06
Index ranges	-10 ≤ h ≤ 10, -15 ≤ k ≤ 15, -29 ≤ l ≤ 30
Reflections collected	31948
Independent reflections	4697 [R_{int} = 0.0596, R_{sigma} = 0.0354]
Data/restraints/parameters	4697/0/280
Goodness-of-fit on F^2	1.080
Final R indexes [I>=2σ (I)]	R_1 = 0.0598, wR_2 = 0.1483
Final R indexes [all data]	R_1 = 0.0653, wR_2 = 0.1524

Table S4: Bond Lengths for 4ab

Atom	Atom	Length/Å	Atom	Atom	Length/Å
N1	C1	1.342(2)	C9	C14	1.501(3)
N1	C5	1.345(2)	C10	C11	1.378(3)
N2	C6	1.275(2)	C11	C25'	1.281(19)
N2	C8	1.418(2)	C11	C12	1.386(3)
N3	C16	1.275(2)	C12	C13	1.388(3)
N3	C18	1.419(2)	C13	C15	1.508(3)
C1	C2	1.397(2)	C16	C17	1.502(3)
C1	C6	1.496(2)	C18	C23	1.405(3)
C2	C3	1.386(3)	C18	C19	1.408(3)
C3	C4	1.382(3)	C19	C20	1.386(3)
C4	C5	1.397(3)	C19	C24	1.506(3)
C5	C16	1.489(2)	C20	C21	1.388(3)
C6	C7	1.503(2)	C21	C22	1.396(3)
C8	C13	1.397(2)	C21	C25	1.503(3)
C8	C9	1.403(3)	C22	C23	1.387(3)
C9	C10	1.391(3)	C23	C26	1.500(3)

Table S5 Bond Angles for 4ab

Atom	Atom	Atom	Angle/˚	Atom	Atom	Atom	Angle/˚
C1	N1	C5	118.26(14)	C25'	C11	C12	124.5(10)
C6	N2	C8	121.84(14)	C10	C11	C12	119.26(17)
C16	N3	C18	121.52(16)	C11	C12	C13	121.51(16)
N1	C1	C2	122.69(16)	C12	C13	C8	118.64(17)
N1	C1	C6	116.46(14)	C12	C13	C15	121.67(16)
C2	C1	C6	120.84(15)	C8	C13	C15	119.68(16)
C3	C2	C1	118.49(17)	N3	C16	C5	117.51(16)
C4	C3	C2	119.30(17)	N3	C16	C17	125.00(16)
C3	C4	C5	118.82(17)	C5	C16	C17	117.47(15)
N1	C5	C4	122.40(16)	C23	C18	C19	120.42(17)
N1	C5	C16	116.92(15)	C23	C18	N3	118.40(16)
C4	C5	C16	120.64(16)	C19	C18	N3	120.92(16)
N2	C6	C1	117.39(15)	C20	C19	C18	119.02(18)
N2	C6	C7	125.32(16)	C20	C19	C24	120.14(18)
C1	C6	C7	117.27(15)	C18	C19	C24	120.84(18)
C13	C8	C9	120.50(16)	C19	C20	C21	121.80(19)
C13	C8	N2	119.39(16)	C20	C21	C22	118.03(18)
C9	C8	N2	119.72(15)	C20	C21	C25	118.9(2)
C10	C9	C8	118.92(16)	C22	C21	C25	123.0(2)
C10	C9	C14	120.88(17)	C23	C22	C21	122.36(18)
C8	C9	C14	120.19(17)	C22	C23	C18	118.30(17)
C11	C10	C9	121.16(18)	C22	C23	C26	122.14(17)
C25'	C11	C10	116.2(10)	C18	C23	C26	119.56(17)